Physica E 134 (2021) 114923

Contents lists available at ScienceDirect

Physica E: Low-dimensional Systems and Nanostructures

journal homepage: www.elsevier.com/locate/physe

Surface optical phonon and multi – phonon transitions in YVO_4: Eu^{3+} nanopowders

J. Mitrić [a,*], N. Paunović [a], M. Mitrić [c], J. Ćirković [b], M. Gilić [a], M. Romčević [a], N. Romčević [a]

[a] Institute of Physics, University of Belgrade, Pregrevica 118, 11080, Belgrade, Serbia
[b] Institute for Multidisciplinary Research, University of Belgrade, Kneza Višeslava 1a, 11030, Belgrade, Serbia
[c] Institute Vinča, University of Belgrade, P.O. Box 522, 11001, Belgrade, Serbia

ARTICLE INFO

Keywords:
Surface optical phonon
Multi
Phonon
Yttrium orthovanadate
Europium
Infrared spectroscopy
uv
Vis spectroscopy

ABSTRACT

In this paper two methods of preparation of yttrium orthovanadate nanopowders were presented: Solid State Reaction (top – down approach) and Solution Combustion Synthesis (bottom – up approach). For starting structural characterization, X – Ray Powder Diffraction (XPRD) and Field Emission Scanning Electron Microscopy (FESEM) were used. We report the change in reflection spectra in europium doped YVO_4 nanopowders with comparison to its bulk analog. In UV–Vis reflection spectra we consider the change in values of band gap in these structures, after resizing it from bulk to nanomaterial. In Far – Infrared (FIR) reflection spectra, we registered the existence of Surface Optical Phonon (SOP) and different multi – phonon processes which alter the reflection spectra of bulk YVO_4. The influence of Eu ions is reflected through multi – phonon processes that occur and are connected with energy transfer from YVO_4 lattice to Eu ions. All IR spectra were modeled using classical oscillator model with Drude part added which takes into account the free carrier contribution. Since our samples are distinctively inhomogeneous materials, we use Effective Medium theory in Maxwell Garnett approximation to model its effective dieletric function.

1. Introduction

Semiconducting nanomaterials, especially nanophosphors have attracted great attention of researchers, due to their wide spectrum of applications in industry, technology as well as in fundamental science. When made in nanorange, phosphor materials exibit enhanced optical properties as against their bulk counterparts, due to quantum size effects and increased surface – to – volume ratio. Yttrium orthovanadate is a widely used red phosphor with many applications in just recent years – in solar cells [1], cancer treatment [2], biotechnology [3], optical imaging [4] etc.

For nanopowders, a valuable tool in the investigation of the structural and optical changes in a material made due to resizing the bulk crystal on nanoscale is the optical spectroscopy – in this case specifically far – infrared and UV – VIS spectroscopy. When excited by UV light, photoluminescence quantum yield of the europium emission in yttrium orthovanadate crystal, goes up to 70% [5]. In YVO_4:Eu^{3+} structure UV radiation excites the vanadate group, which has the ability of efficient excitation transfer to the europium ions (Fig. 1).

When irradiated with UV radiation, three major steps occur in the excitation and emission process in YVO_4:Eu^{3+} structure. First step is the absorption of UV light by $(VO_4)^{3-}$ groups. Then, thermal activated energy, which comes from the UV excitation source, migrates through the vanadate sub – lattice, inducing the transfer of excited energy to europium ions. In the end, strong red ($^5D_0$ – $^7F_2$) and orange ($^5D_0$ – $^7F_1$) emission due to de – excitation process of excited europium ions occur [6].

One of the important properties of semiconductors is their band gap. Studying the band gap of semiconductors is important for interpreting their structural and optical properties and it is of a great importance examining its expansion in order to understand their properties. Application of semiconductors is in large level determined by their band gap width. Bulk semiconductors are usually very limited in their application due to their small and indirect band gap. Bulk crystal is set up of a large number of atoms and molecules, with a number of adjacent energy levels, which form bulk electronic bands. With the reduction of particle size to a nano level, where every particle is made up out of a small number of atoms or molecules, the number of overlapping orbitals decreases, and the eventually width of the band gap of a nanomaterial gets narrower when compared to bulk crystal (this means that there will be

* Corresponding author.
E-mail address: jmitric@ipb.ac.rs (J. Mitrić).

https://doi.org/10.1016/j.physe.2021.114923
Received 7 May 2021; Received in revised form 3 August 2021; Accepted 4 August 2021
Available online 14 August 2021

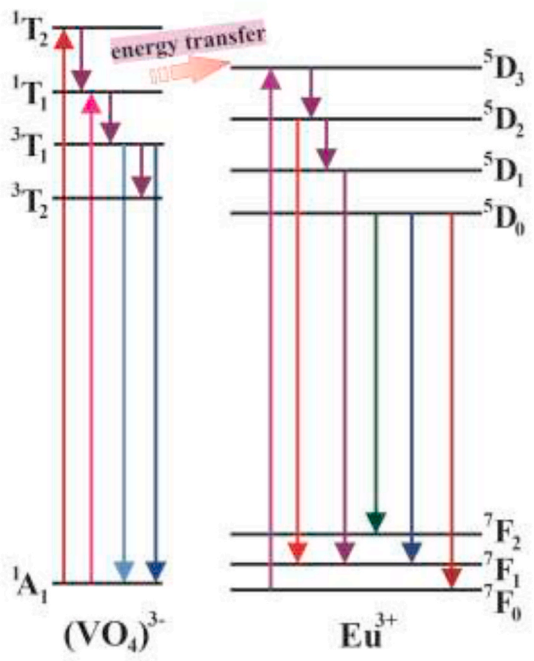

Fig. 1. Energy levels and energy transfer model of Eu^{3+} ion and $(VO_4)^{3-}$ tetrahedron in YVO4.

an increase of energy between valence and conduction band). This is the reason why nanomaterials have wider band gap compared to their bulk counterparts. The larger the band gap (i.e. forbidden region), the greater the restriction of the electron movement will be. This is well known as the *quantum size effect*. As a consequence of size reduction, there is a shift of absorption spectrum of nanomaterials towards the lower wavelengths, known as a *blue shift*.

In bulk crystals, bulk longitudinal (ω_{LO}) and transversal (ω_{TO}) optical phonon frequency occur. In crystals with relatively small dimensions, a new frequency appears – Surface Optical Phonon (SOP) frequency (ω_{SOP}) which is located between the ω_{LO} and ω_{TO} frequency. That means that due to effects of dimension, in addition to the modes of infinity lattice, surface modes will be manifested. And in the case of crystals with extremely low dimensions, only the surface mode perseveres.

Different types of interactions with electromagnetic radiation takes an important place in semiconductors. On one side, we have investigated electron – phonon interaction in ceramic nanopowders [7]; surface optical phonon – plasmon in thin films [8]. Besides that, we have studied damping influence on interaction appearance [9], plasmon – impurity local phonons [10], as well as plasmon – different phonons interactions [11].

A special attention should be given to the choice of method for nanopowder preparation, because nanostructured samples with good crystallization and homogenous particle size exhibit extraordinary properties different from their bulk analogs. At the same time, a very important thing for their application in industry and technology is finding a fast, cheap and reproducible technique for obtaining fine nanophosphors.

In this paper two types of methods were presented. One, the top – down approach, *Solid State Reaction Method* (SSR), (which implies extensive milling), which is a classical ceramic method and the other, bottom – up approach, *Solution Combustion Synthesis* (SCS). Top down approaches have advantages like large scale production and deposition over a large substrate; also, with these techniques, chemical purifications are not required. Disadvantages of top – down methods are varied particles shapes or geometry, different impurities (stresses, defects and imperfections); also, one must be very careful not to have broad size distribution of particles. Bottom – up approaches, on the other hand, offer ultra – fine nanoparticles, with controlled deposition and narrow size distribution. Unlike the previous techniques, bottom – up approaches do not offer large scale production so easily, and require chemical purification. Therefore, we have chosen one technique from both approaches so they can be compared. In this paper we offer two simple, fast, cheap and yet reproducible techniques for yttrium orthovanadate nanopowder preparation.

1.1. Bulk crystal of YVO_4

Yttrium orthovanadate crystal has a zircon – type of structure, and crystalizes in 141. Space group, $I4_1/amd$ shown in Fig. 2. In this structural type, Y ions occupy ***4a*** crystallographic (Wyckoff) site with coordinates $[[0, 3/4, 1/8]]$.

V ions occupy ***4b*** crystallographic site, and coordinates $[[0, 1/4, 3/8]]$; while O ions occupy ***16h*** crystallographic site, with coordinates $[[0, y, z]]$.

This structure belongs to 4/mmm Laue class, where fourfold axis is a unique symmetry operation and has an expressed anisotropy of physical properties. V ions are in tetrahedral surrounding of O ions, while the surrounding of Y ions is made of oxygen coordination sphere with eight O ions which form a highly distorted cube.

From a group – theory analysis [12] it is known for this type of symmetry with two chemical formulas in the primitive cell ($I4_1/amd$ – D_{4h}^{19}) to have following modes in the center of the Brillouin zone at the Γ point: $\Gamma(k = 0) = 2A_{1g} + 5E_g + 4B_{1g} + 1B_{2g} + 4A_{2u} + 5E_u + 1A_{2g} + 1A_{1u} + 1B_{1u} + 2B_{2u}$. E_u and A_{2u} modes show dipole moments oriented perpendicular and along the c directions, respectively; and four out of five E_u modes are infrared active.

Infrared reflection spectrum of bulk YVO_4 can be found in the literature [13]. In the measured reflectivity spectra, two sharp features at the lowest frequency can be found, and they correspond to the unscreened infrared – active optical phonon modes. This spectrum is characterized with four peaks of which three are easily seen, while the fourth is a shoulder of the second reflectivity band, and it is more evident at lower temperatures. Since bulk YVO_4 has no metallic contribution (i.e. free carrier contribution), the Lyddane – Sachs Teller (LST) relation (Lorenz oscillator model) can be an optimal model to analyze reflection spectra and to model an appropriate dieletric function of a material.

In this paper we report the change in reflection spectra of europium

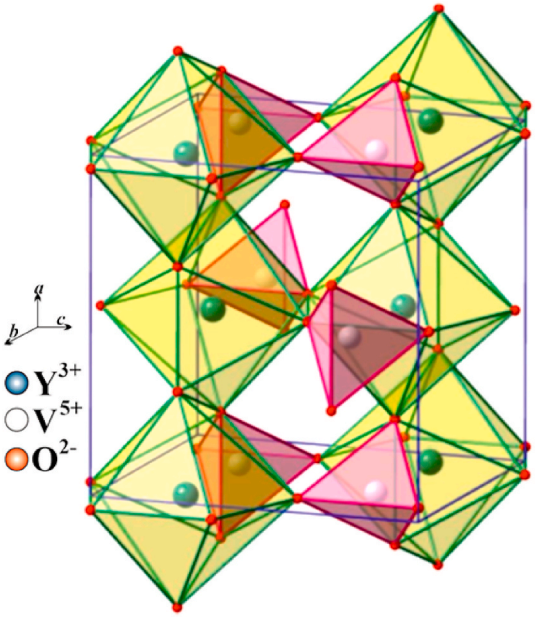

Fig. 2. Crystal structure of YVO4.

doped YVO_4 nanpowders with comparison to its bulk analog. In UV – VIS reflection spectra we consider the change in values of a band gap of europium doped YVO_4 when it is resized from bulk to nanomaterial. In IR reflection spectra we carry out phonon investigation in order to explain the change in optical properties of investigated nanopowders. We show the existence of surface optical phonon (SOP) and different phonon processes which alter the reflection spectra of bulk YVO_4. Full characterization of materials is made with X – Ray Powder Diffraction (XRPD) and Field Emission Scanning Electron Microscopy (FESEM).

2. Sample preparation and characterization methods

Nanopowders prepared by SCS were obtained using stoichiometric quantities of starting chemicals $Y(NO_3)_3{\cdot}6H_2O, NH_4VO_3, NH_4NO_3$ and $Y(NO_3)_3{\cdot}6H_2O$, purchased from ABCR with the purity of 99.99%. Urea was purchased from Sigma – Aldrich. Eu^{3+} concentration was 1%. 4.8 g of NH_4NO_3 and 3.003 g of urea, $(NH_2)_2CO$ which were used as an organic fuels were added to a dry mixture of 0.357 g $Eu(NO_3)_3{\cdot}\ 6H_2O$, 4,676 g of NH_4VO_3 and 15.32 g of $Y(NO_3)_3{\cdot}6H_2O$. Then, mixture was combusted with the flame burner at $\sim 500^{\circ}C$. Then, the solid solution starts to act like cloud – shape mixture which then was annealed in air atmosphere at $1200^{\circ}C$ for 2 h. The annealing of material offers full crystallinity. This sample was labeled as **YVS**.

Solid state reaction procedure was performed using stoichiometric quantities of starting chemicals, then powdered and baked on $900^{\circ}C$ for 5 h. Starting chemicals, Y_2O_5, Y_2O_3 and Eu_2O_3 with purity of 99.99% were purchased from ABCR. Concentration of Eu ions was 1%. This sample was labeled as **YVC**. Both samples, YVS and YVC, were made in a series of 5 samples, and every measurement is an average of these 5 samples.

These two simple, but yet reproducible and efficient methods provide two morphologically different samples. In this way methods can be compared and analyzed.

Structural characteristics of yttrium orthovanadate nanopowders were obtained using Philips PW 1050 diffractometer equipped with a PW 1703 generator, 40 kV × 20 mA, using Ni filtered Co Kα radiation of 0.1778897 nm, at room temperature. 15–85° range was used during 2 h, with a scanning step of 0.05° and 10s scanning time per step.

Morphologies of prepared samples were examined by Field Emission Scanning Electron Microscopy using FEI Scios 2 with an acceleration voltage between cathode and anode 15 kV.

All UV–Vis reflectance spectra were recorded in the wavelength range of 200–1200 nm on the Shimadzu UV – 2600 spectrophotometer equipped with an integrated sphere. The reflectance spectra were measured relative to a reference sample of $BaSO_4$.

The infrared reflectivity measurements were performed at room temperature. BOMEM DA – 8 Fourier – transform infrared spectrometer was used. A Hyper beamsplitter and DTGS (deuterated triglycine sulfate) pyroelectric detector were used to cover the wave number region 80–650 cm^{-1}. Spectra were collected with 2 cm^{-1} resolution with 500 interferometer scans added for each spectrum.

2.1. X – ray powder diffraction

Results for YVC and YVS are shown in Fig. 3. The diffractograms confirm that both samples are monophased and that they crystallized in zircon – type of structure. All reflections are in good agreement with JCPDS card 17–0341. Also, all samples show no other reflections other than ones who originate from YVO_4 structure. Since Eu^{3+} concentration in these samples is 2%, one cannot be identified by XRD. Crystallite sizes are 53 nm and 58 nm for YVC and YVS, respectively. Crystallite sizes were determined using Debye Scherrer formula. This formula gives value of average crystallite size, and from our calculations the deviation is around 5 nm. To reduce this error, series of every sample were made (5 from each) to reduce the influence of chemical modification and other processing conditions). Even though Debye Scherrer is a rough method for determining crystallite size and one could use other methods for determining this value, like Williamson – Hall analysis which could in some way reduce this problem, this would suggest to rely on some other assumptions which could add up to an error. Crystallite size for sample YVC is smaller than one obtained in YVC. This was expected because of method of preparation. YVC was prepared using Solid State Reaction Method, which includes rather aggressive milling, and therefore results in smaller crystallite size than sample YVC, which was obtained with Solution Combustion Synthesis.

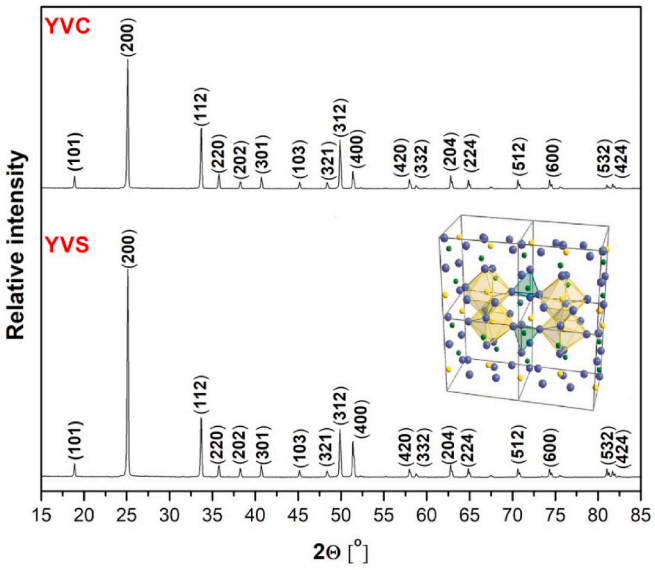

Fig. 3. XRD patterns of europium doped yttrium – orthovanadate nanopowder prepared by Solid State Reaction Method (YVC) and Solution Combustion Synthesis (YVS).

2.2. Field emission scanning electron microscopy

FESEM photographs are shown in Figs. 4 and 5, for YVS and YVC respectively; with 10 000 × and 35 000× magnification. Particle sizes are 2 m and 3 μm, for YVC and YVS, respectively. These values are much larger than the ones obtained with XRD. Reason for this is crystallite agglomeration. Regardless of agglomeration, trend in crystallite size between two methods of preparation remains the same as in crystallite sizes determined by XRD. One more thing must be noticed, and that is difference in crystallinity between samples. As can be seen from Figs. 4 and 5, sample YVC is more crystalline than YVS, which has more of a cloud – shape structure. This was marked with yellow rectangles in Figs. 4 and 5. On a larger scale, both samples consist of clearly defined and separated grains which can be seen on right hand side of Figs. 4 and 5.

3. Results and discussion

3.1. UV – VIS spectroscopy

In this section we investigated optical UV–Vis reflection spectra of europium – doped yttrium orthovanadate nanopowders. Special attention was given to obtaining band gap values. Band gap values were obtained using Tauc plot [14]. It is important to have information about band gap values, because band structure is responsible for the wide range of electrical characteristics. Tauc, Davis and Mott [15] have proposed an expression:

$$\alpha h\nu = A\left(h\nu - E_g\right)^{1/n} \quad (1)$$

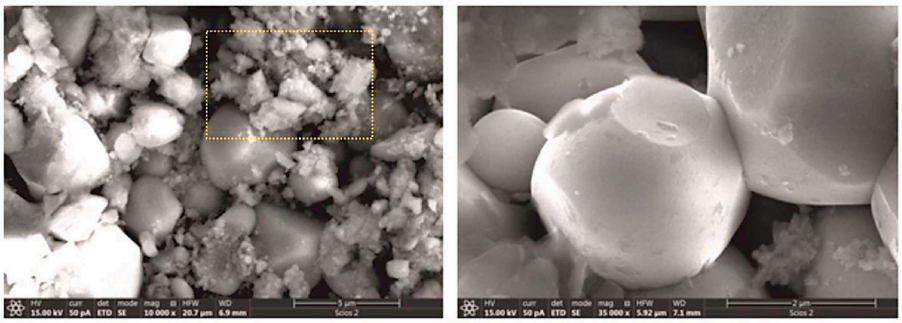

Fig. 4. FESEM photographs of europium doped yttrium – orthovanadate nanopowder prepared by Solid State Reaction Method (YVS).

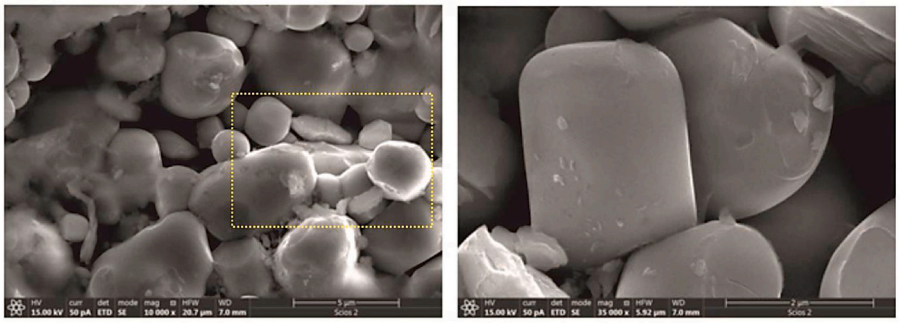

Fig. 5. (a) FESEM photographs of europium doped yttrium – orthovanadate nanopowder prepared by Solid State Reaction Method (YVC).

where α is the absorption coefficient (which is a property of a material; it defines the amount of light absorbed by it); h is the Planck's constant and $h\nu$ is the photon energy. A represents transition probability constant (which depends on the effective mass of the charge carriers in the material) and E_g is the band gap. Number n defines the nature of transition. If transition is direct, n equals 1/2 and 3/2, for the allowed and forbidden transitions, respectively. In the case of indirect transitions, n is 2 for allowed and 3 for forbidden transitions. In our case n is 3/2.

Then, the obtained diffuse reflectance spectra are converted to Kubelka – Munk function [16]:

$$\alpha = \frac{(1-R)^2}{2R} \tag{2}$$

where R is a reflectance value. Using Eqs. (1) and (2), we obtain $(\alpha h\nu)^{1/n}$ vs. $h\nu$ plot. By extrapolating the linear portion of mentioned dependence to the energy axes at the $(\alpha h\nu)^{1/n} = 0$ value, the band gap value is obtrained – the intercept of the plot with x – axe gives the value of band gap. The results obtained with UV – VIS spectroscopy, UV – VIS reflectance and diffuse reflectance Kubelka – Munk spectra for YVS and YVC are presented in Figs. 6 and 7 respectively.

From Table 1 values of calculated band gap for europium doped yttrium orthovanadate nanopowders prepared by two methods, as well as literature data for bulk YVO_4 were presented. With regard to section 2 where it was explained how band gap values increases with decreasing grain size, we got matching results. Namely, we got two values of band gap for samples made with two methods, YVC and YVS: 3, 55 eV and 3,17 eV, respectively. Since crystallite size of YVC (53 nm) is smaller than in YVS (58 nm), it is expected that the band gap value will be greater for YVC, due to quantum size effect described earlier. Both E_g values for nanophosphors are greater that the E_g value for bulk crystal YVO_4, which is expected. With this we conclude that Solid State Reaction Method provides samples with higher band gap values that samples prepared by Solution Combustion Synthesis.

When under the UV–Vis radiation, three major steps occur in YVO_4: Eu^{3+}: 1. absorbance of radiation by $(VO_4)^{3-}$ groups; 2. transfer of the excited energy to Eu^{3+} ions which migrated through vanadate sublattice; and 3. red emission induced by de – excitation process of excited Eu^{3+} ions. This was represented in Fig. 1.

Peak at around 272 nm originates from absorption of $(VO_4)^{3-}$ groups [17]. According to the literature, this peak is an attribution to charge transfer from oxygen ligands to the central vanadium atom in $(VO_4)^{3-}$ group. In that way, UV–Vis spectra from Figs. 6a and 7a prove there is an energy transfer between $(VO_4)^{3-}$ and Eu^{3+} ions. Peak at 343 nm originates from $(VO_4)^{3-}$ in the lattice [18]. Peak at 272 in YVS is clearly seen. On the other hand, in YVC sample, splitting of 272 mode is obvious. The mode split because reflectance values cannot go below zero values; and increase in intensity of reflectance compared to YVS is caused by multi – phonon processes which seem to be more dominant in YVC rather than in YVS.

In one of our previous papers [19] it is shown how Eu ions exchange with of Y ions, and without any significant disturbance of symmetry take place in YVO_4 structure. Clearly, Eu ions have more influence in YVC sample, which has more crystallinity and smaller crystallite size, and are more efficiently distributed throughout the YVC sample. More evidence on multi – phonon processes which are present in YVC will be shown more clearly using Infrared Spectroscopy.

Results like this also confirm that these materials are suitable for many optical devices. Following our previous research [20] these phosphors represent an excellent hosts for optical excitation and emission of europium. Also, since the samples were made using two different techniques on different temperatures (500 and 900 °C), a certain evidence of thermal stability on emission quantum yield and lifetime was shown which is in good agreement with the literature [21].

3.2. Infrared spectroscopy

Subject of this paper are distinctively inhomogeneous materials. They are built out of embedded components in a matrix, and every one of them has its own macroscopic properties. A macroscopic property can

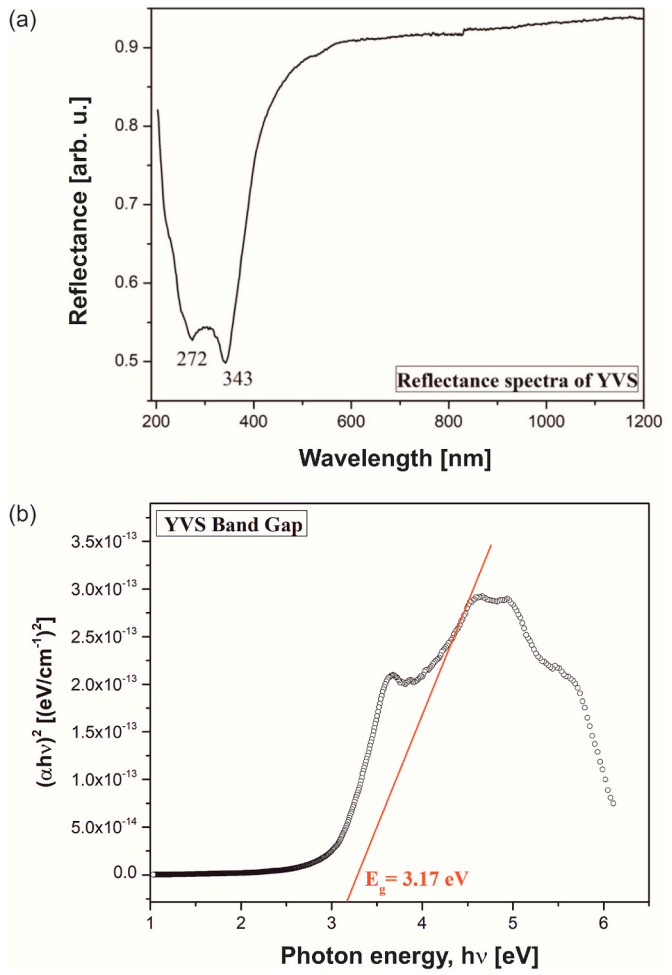

Fig. 6. (a) UV – VIS reflectance spectra of europium doped yttrium – orthovanadate nanopowder prepared by Solid State Reaction (YVC). (b) Kubelka – Munk plot for europium – doped yttrium – orthovanadate nanopowder prepared by Solid State Reaction (YVS).

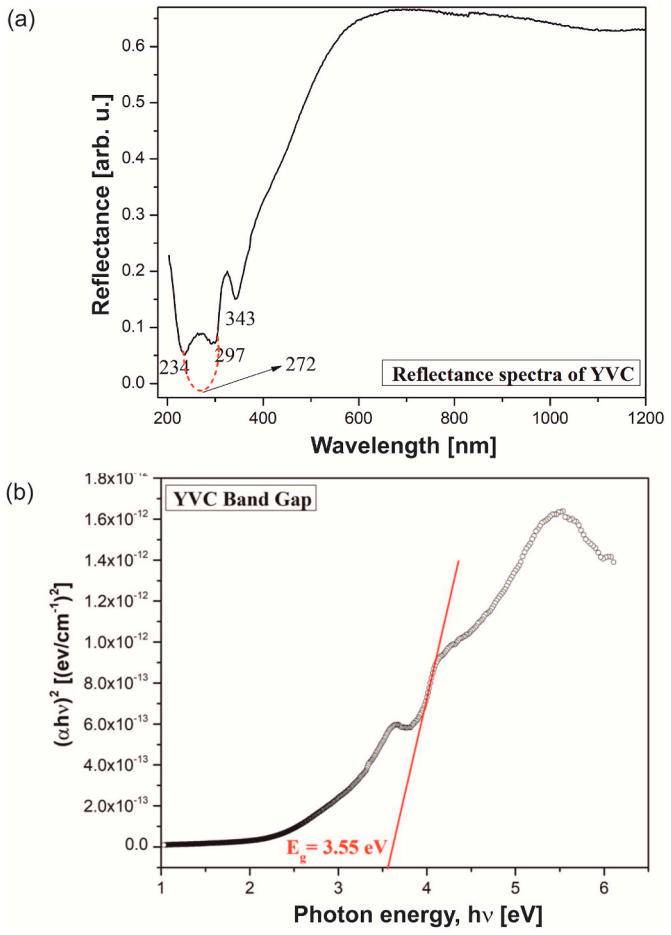

Fig. 7. (a) UV – VIS reflectance spectra of europium doped yttrium – orthovanadate nanopowder prepared by Solution Combustion Synthesis (YVC). (b) Kubelka – Munk plot for europium – doped yttrium – orthovanadate nanopowder prepared by Solution Combustion Synthesis.

be attributed to every component of this material, as well as to a matrix. For example, this can be a dielectric permittivity. A medium where dielectric permittivity of every component and its surrounding (matrix) can be substituted with one value of dielectric permittivity, *an effective dielectric permittivity*, is called an effective medium, and theory which describes this is known as Effective Medium Theory. In other words, within this model, a heterogeneous system can be seen, from a bigger scale, as a homogeneous system, with its own properties which are often called effective properties, with one important fact: on a scale comparable with the dimensions of the system constituents, the system cannot be regarded as a homogeneous medium. Theory of effective medium has several approximations [22], of which two are most common: Maxwell Garnet and Brugemann approximation. The first one implies that constitutive parts of one medium are very well separated out of matrix they've been embedded in, and that there is no electrostatic interactions between them. On the other hand, Brugemann approximation describes systems where constitutive parts cannot be separated out of their surroundings.

When visible light, λ, interacts with a material described above, where its nanoparticles have characteristic size d, and dielectric function ε_2, which are randomly distributed in a matrix with a dielectric constant ε_1, in the limit $\lambda \gg d$, the heterogeneous composite can be treated as a homogenous, and this system can be described with Effective Medium Theory. Since the samples we investigate are well defined, spherical and separated nano grains (as seen in Figs. 4 and 5), we use Maxwell Garnet

Table 1
Band gap values for YVC, YVS and literature data for bulk YVO_4 bulk crystal.

YVC	YVS	YVO_4 bulk (literature) [22]
3.56 eV	3.16 eV	2.85 eV

model for the present case. Following postulates of this approximation, for the effective permittivity of so called homogeneous medium we get [23]:

$$\varepsilon_{eff} = \varepsilon_1 + 3f_1\frac{\varepsilon_1(\varepsilon_2 - \varepsilon_1)}{\varepsilon_2 + 2\varepsilon_1} \tag{3}$$

where ε_2 is a dielectric permittivity of nanoparticles located randomly in a homogeneous environment with dielectric permittivity ε_1, which is, in our case, air; and occupy a volume fraction f (so called filling factor).

For modeling dielectric permittivity of above described nanoparticles, we have used a classical oscillator model with Drude part added (second addition in Eq. (3)) which takes into account the free carrier contribution [24].:

$$\varepsilon_2(\omega) = \varepsilon_\infty\left(\prod_{k=1}^{n}\frac{\omega_{LO}^2 - \omega^2 + i\gamma_{LO}\omega}{\omega_{TO}^2 - \omega^2 + i\gamma_{TO}\omega} - \frac{\omega_P^2}{\omega(\omega - i\tau^{-1})}\right) \tag{4}$$

where ε_∞ is a bound charge contribution (assumed to be constant), transverse and longitudinal frequencies are noted with ω_{TO} and ω_{LO}, γ_{TO} and γ_{LO} are their damping coefficients, ω_P is plasma frequency and free

carrier relaxation time is marked by τ.

Calculated spectra were obtained by a fitting procedure using a previously described model which is represented with solid lines in Figs. 8 and 9. Using the least – square fitting procedure of the experimental (R_{exp}) and theoretical (R_{th}) reflectivity, at q arbitrarily taken points, the parameter adjustment was carried out, automatically.

$$\delta = \sqrt{\frac{1}{q}\sum_{j=1}^{q}\left(R_{exp} - R_{th}\right)^2} \tag{5}$$

Minimalization of δ was carried out until it met the conditions of commonly accepted experimental error of less than 3%.

Theoretical model in Figs. 8c and 9, show excellent match with the experimental results, for YVS and YVC samples, respectively. In Table 2, best fitting parameters are presented. In Eq. (4), transversal optical frequency, ω_{TO}, was precieved as the characteristic frequency for a given material. As regards to spectra from Fig. 8a and 8b, they show the procedure, step by step, in order to get the best fit presented in Fig. 8c. Model used in Fig. 8a did not take into account the existence of SOP. Actually, this model suits the bulk structure of YVO_4 the best, when there's no SOP [25]. After we took this into account, we notice that, when bulk YVO_4 was resized to nanoscale, wide mode on the highest frequencies in bulk spectrum of YVO_4 [13] split into two modes. Since this was modeled with dielectric function which takes into account the existence of SOP, we conclude that the reason for splitting this wide

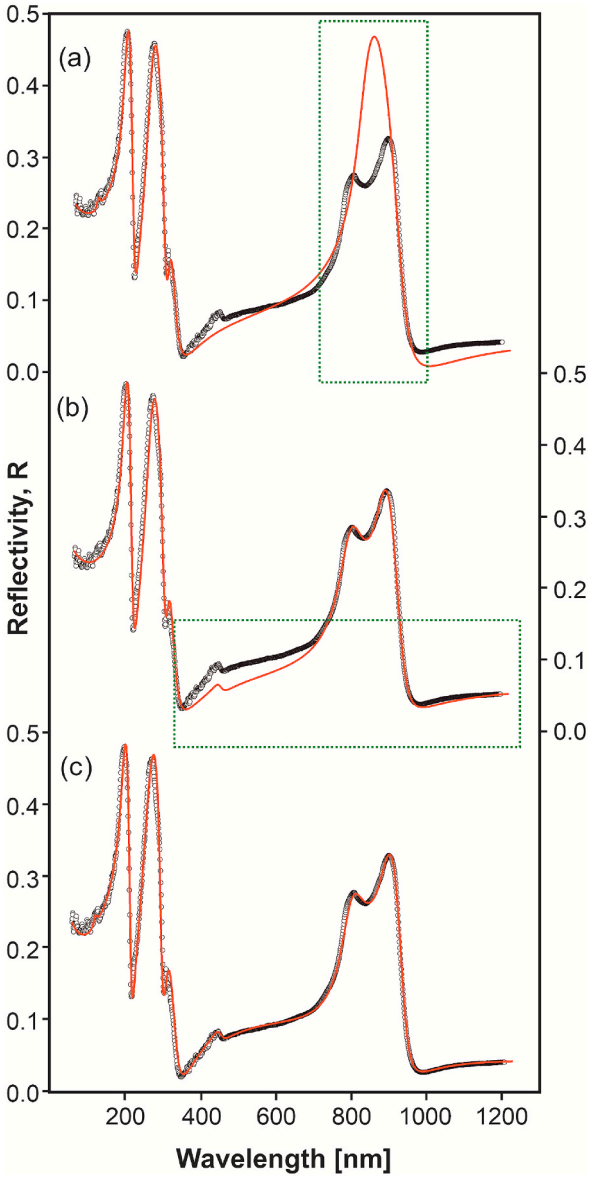

Fig. 8. Infrared reflection spectra of YVO_4 nanopowders prepared by Solution Combustion Synthesis (sample YVS). Experimental spectra are presented by open circles, while solid red lines are calculated spectra obtained by a fitting procedure based on the model given by Eqs. (3) and (4). Spectrum (a) shows fitting procedure without taking into account SOP phonons, (b) spectrum without taking into account multiphonon processes and (c) IR reflection spectrum of YVS when SOP phonons and multiphonon process were considered.

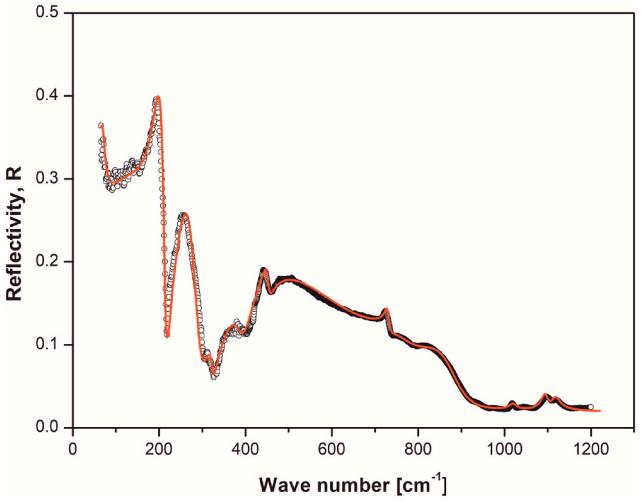

Fig. 9. Infrared reflection spectra of YVO4 nanopowders prepared by Solid State Reaction (sample YVC). Experimental spectra are presented by open circles, while solid red lines are calculated spectra obtained by a fitting procedure based on the model given by Eqs. (3) and (4).

Table 2
Best fitted parameters of IR reflection spectra for YV, YVC and YVC; bulk literature data and their assignments.

	YVC [cm^{-1}]	YVS [cm^{-1}]	Bulk YVO4 (Literature data) [cm^{-1}] [13]	Assignment
ε_∞	1.8	2.25	4.0	
F	0.79	0.93	1	
Γ_P	85	200		
ω_P	100	89		Plasmon frequency which plays role of ω_-
ω_{TO3}	212	198	195	E_u mode, IR active
ω_{LO3}	214	219	220	
ω_{TO4}	234	259	263	E_u mod, IR active
ω_{LO4}	292	300	309	
ω_{TO5}	321	311	309	E_u mod, IR active
ω_{LO5}	323	337	311	
ω_{TO6}	397	–		Multiphonon processes
ω_{LO6}	393	–		
ω_{TO7}	400	470		
ω_{LO7}	645	650		
ω_{TO8}	450.5	452		
ω_{LO8}	452	454		
ω_{TO9}	730.2	–		
ω_{LO9}	731	–		
ω_{TO10}	759	794	780	SOP formation. E_u mod, IR active
ω_{LOSOP}	863	890		SOP phonon
ω_{LO10}	887	935	930	
ω_{TO11}	1020	–		Multiphonon processes
ω_{LO11}	1021	–		
ω_{TO12}	1093.5	–		
ω_{LO12}	1096	–		
ω_{TO13}	1116	–		
ω_{LO13}	1117.5	–		

mode is occurrence of SOP mode in these structures. After including SOP modes into reflection spectra of nanostructures, we still have slight differences between experimental and theoretical results (Fig. 8b) at frequency between two sharp modes at lowest, and one wide mode at highest frequencies.

Reasons for this slight difference presented in Fig. 8b are different multi – phonon processes, with frequencies obtained in Table 2. After we took this into account, we got excellent match of theoretical and experimental results, shown in Fig. 8c.

From this we conclude that influence in reflection IR spectra in majority comes from SOP mode and not from multi – phonons. Still, when we compare two spectra from 8c and 9, we do see differences, which originate from different contributors to reflection IR spectra. In sample made with Solution Combustion Synthesis (YVS), the contribution of SOP is greater than in samples made with Solid State Reaction (YVC). Yet, in sample YVC, influence of multi – phonon contributors is greater than in YVS which is also shown in UV–Vis measurements. We see that from Table 2, for the wavenumbers greater than 1020 cm^{-1}, where we modeled multi – phonon modes for YVC and not for YVS, because of the greater influence of SOP in this sample which completely covered possible multi – phonon processes in YVS. From all of this, we can say that, when we compare to nanopowders prepared with two different methods, one can say that for YVS, influence of SOP mode dominates, and for sample YVC, multi – phonon modes dominate over SOP modes.

Now, let us discuss the results obtained in Table 2. In Eq. (3) we have defined the parameter called filling factor. It is a parameter which describes the volume fraction occupied by the nanoparticle (or nanoparticle aggregates) in the surrounding medium. In Table 2, filling factors of prepared nanopowders, YVC and YVS, together with value for bulk crystal YVO_4 are presented. Intensity and shape change of SOP modes presented in Figs. 8 and 9 (described with Eq. (4)) are notably affected by variation of filling factor, f.

In our case, position of SOP modes maxima directly follows the change in filling factor. Position of SOP modes frequencies are obtained from Eq. (6) [26], and the results are presented in Fig. 10.

$$\omega_{SOP} = \max\left(I_m\left(-\frac{1}{\varepsilon_{eff}}\right)\right) \tag{6}$$

In bulk crystal YVO_4 [13], at room temperature, four modes in infrared reflection spectra have been detected at 195, 263, 311 and 780 cm^{-1}. These modes are separated into internal (motions of the tetrahedral VO_4) and external (translations and rotations of the VO_4 tetrahedron). All of these modes, as expected, are shifted after resizing bulk to nanomaterial to 212, 234, 323 and 759 cm^{-1} for YVC, and to 198, 259, 337 and 794 cm^{-1} for YVS, respectively. Appearance of new phonons is due to break – down of the selection rules, as a consequence of resizing of the bulk crystal to nanostructure. Some modes occur due to appearance of surface optical phonon mode and some due to multi – phonon processes (one is, as we said, more dominant in YVS and other in YVC) in addition to modes which occur owing to Eu ion and its interaction with YVO_4 lattice. All of the modes are represented and assigned in Table 2.

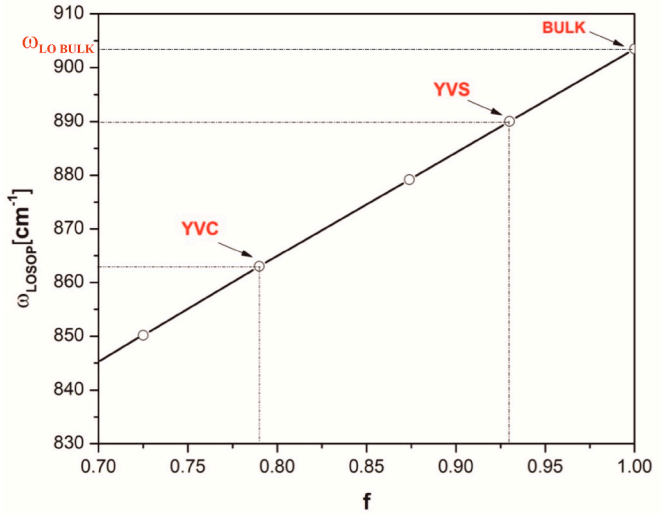

Fig. 10. Surface Optical Phonon mode position vs. filling factor.

Based on these results, it is clear that filling factor of prepared nanopowders depends on method of preparation, but yet it has a linear dependence of occurred surface optical phonon frequency. Also, SOP mode has the role of the LO phonon which we have also showed in our earlier works in different nanostructures [8].

Vibrational spectroscopy of nanostructures for discovering surface optical phonons represents an extremely active and exciting field with many possibilities for scientific and technological development. This arising new phenomena offer not only new perspective for material characterization, but also a fundamental understanding of processes at nanoscale. Better understanding of phonon properties of phosphors shown in this paper leads to wide application of these nanostructured materials for nanophosphor coatings [27], biomedical application [28], luminescence efficiency [29] etc. Also, discovery of surface phonons in these materials offer great use in heteronanostructures [30] to enhance the photoluminescence properties.

On the other side, multiphonon processes have been investigated for the first time in this nanostructured orthovanadate. Understanding multiphonon processes and charge transfers within a phosphor structure leads to its better application in self – assembled quantum dots [31] and different luminescent materials [32].

4. Conclusion

In this paper we showed two methods of preparation of yttrium orthovanadate nanopowders, Solution Combustion Synthesis and Solid State Reaction Method. Samples prepared by Solution Combustion Synthesis offer slightly bigger crystallite size, and therefore smaller width of band gap compared to samples prepared by Solid State Reaction Method, which provides samples with band gap up to 3.56 eV which was obtained using UV–Vis spectroscopy. Splitting of 272 nm mode from UV–Vis spectra for sample made by Solid State Reaction Method gives an indication of more dominant multi – phonon modes in this sample rather than in one made by Solid Combustion Synthesis. This was caused by doping and transfer of excited energy which migrates through vanadate sublattice to Eu ions; and after causes red emission induced by de – excitation process of excited Eu ions. For modeling Infrared Reflection spectra of both samples, Effective Medium Theory in Maxwell Garnett approximation was used and classical oscillator model, with Drude part added which takes into account concentration of free carriers. We showed that in both samples characteristic frequency of Surface Optical Phonon occurs as a consequence of resizing bulk crystal to nano scale. Also, that SOP has greater influence in sample prepared by Solution Combustion Synthesis, while in sample prepared by Solid State Reaction Method multi – phonon modes are more dominant and cover SOP modes. This was a confirmation of previous UV–Vis results. Since change in intensity and shape of SOP modes depends on variation of filling factor, we have considered the values of filling factor and its dependence on SOP mode position and came to a conclusion that SOP frequency has a linear dependence on filling factor, where SOP mode plays a role of LO phonon. All results obtained, show not only occurrence of nanoscale phenomena – surface optical phonon and multiphonon processes in YVO_4:Eu^{3+} nanostructures, but its potential use in wide fields of science and technology.

Declaration of competing interest

The authors declare that they have no known competing financial interests or personal relationships that could have appeared to influence the work reported in this paper.

Acknowledgments

The authors acknowledge funding provided by the Institute of Physics Belgrade through the grant by the Ministry of Education, Science, and Technological Development of the Republic of Serbia.

References

[1] T. Voitenko, S.A. Nedilko, K. Savva, M. Androuulidaki, S.G. Nedilko, E. Stratakis, O. Chukova, A. Papadopoulos, Deposition of luminiscent vanadate nanoparticles on silicon solar cells, in: IEE 40th International Conferece on Electronics and Nanotechnology (ELNANO), Kyiv, Ukraine 251 – 254, 2020.
[2] D. Hu, D. Li, X. Liu, Z. Zhou, J. Tang, Y. Shen, Vanadium – based nanomaterials for cancer diagnosis and treatment, Biomed. Mater. (2020) in press.
[3] D. Dosev, M. Nichkova, I.M. Kennedy, Inorganic lanthanide nanophosphors in biotechnology, J. Nanosci. Nanotechnol. 8 (3) (2008) 1052–1067 (16).
[4] L.P. Singh, N.V. Jadhav, S. Sharma, B.N. Pandey, S.K. Srivastava, R. S. Ningthoujam, Hybrid nanomaterials YVO_4:Eu/Fe_3O_4 for optical imaging and hyperthermia in cancer cells, J. Mater. Chem. C 3 (2015) 1965–1975.
[5] W.L. Wanmaker, A. Bril, J.W. Vrugt, J. Broos, Luminiscent properties of Eu – activated phosphors of the type AIIIBnOn, Philips Res. Rep. 21 (1966) 270.
[6] J. Su, X. Mi, J. Sun, L. Yang, C. Hui, L. Lu, Z. Bai, X. Zhang, Tunable luminescence and energy transfer properties in YVO4:Bi^{3+}, Eu^{3+} phosphors, J. Mater. Sci. 52 (2) (2017) 1–11.
[7] J. Mitrić, J. Križan, J. Trajić, G. Križan, M. Romčević, N. Paunović, B. Vasić, N. Romčević, Structural properties of Eu3+ doped Gd2Zr2O7 nanopowders: far – infrared spectroscopy, Opt. Mater. 75 (2018) 662–665.
[8] J. Mitrić, N. Paunović, M. Mitrić, B. Vasić, U. Ralević, J. Trajić, M. Romčević, W. D. Dobrowolski, I.S. Yahia, N. Romčević, Surface optical phonon – plasmon interaction in nanodimensional CdTe thin films, Physica: Low Dimens. Syst. Nanostruct. 104 (2018) 64–70.
[9] N. Romčević, M. Romčević, W.D. Dobrowolski, L. Kilanski, M. Petrović, J. Trajić, B. Hadžić, Z. Lazarević, M. Gilić, J.L. Ristić – Đurović, N. Paunović, A. Reszka, B. J. Kowalski, I.V. Fedorchenko, S.F. Marenkin, Far – infrared spectrscopy of $Zn_{1-x}Mn_xGeAs_2$ single crystals: plasma damping influence on plasmon – phonon interaction, J. Alloys Compd. 649 (2015) 375–379.
[10] N. Romčević, J. Trajić, T.A. Kuznetsova, M. Romčević, B. Hadžić, D.R. Khokhlov, Far – infrared study of impurity local modes in Ni – doped PbTe, J. Alloys Compd. 442 (2007) 324–327.
[11] J. Trajić, M. Romčević, M. Romčević, V.N. Nikiforov, Mater. Res. Bull. 42 (2007), 2201–2192.
[12] C. Pecharroman, M. Ocana, P. Tartaj, C.J. Serna, Optical constants of tetragonal and cubic zirconias in the infrared, Mater. Res. Bull. 29 (1994) 417.
[13] C.Z. Bi, J.Y. Ma, J. Yan, X. Fang, D.Z. Yao, B.R. Zhao, X.G. Qiu, Far – infrared optical properties of YVO_4 single crystal, Eur. Phys. J. B 51 (2006) 167–171.
[14] P. Makula, M. Pacia, W. Macyk, How to corretly determine the band gap energy of modified semiconductor photocatalysts based on UV – Vis spectra, J. Phys. Chem. Lett. 9 (23) (2018) 6814–6817.
[15] X. Li, H. Zhu, J. Wei, K. Wang, E. Xu, Zh Li, D. Wu, Determination of band gaps of self – assembled carbon nanotube films using Tauc/Davis – Mott model, Appl. Phys. A 97 (2009) 341–344.
[16] P. Kubelka, F. Munk, Ein Beitrag zur Optik der Farbanstriche, Zeits F. Teck. Physik. 12 (1931) 593–601.
[17] H. Wang, O. Odawara, H. Wada, Facile and chemically puyre preparation of YVO4: Eu3+ colloid with novel nanostructures via laser ablation in water, Sci. Rep. 6 (2016) 20507.
[18] J. Su, X. Mi, J. Sun, L. Yang, C. Hui, L. Lu, Z. Bai, X. Zhang, Tunable luminescence and energy transfer properties in YVO4:Bi^{3+}, Eu^{3+} phosphors, J. Mater. Sci. 2 (52) (2017).
[19] J. Mitrić, U. Ralević, M. Mitrić, J. Ćirković, G. Križan, M. Romčević, M. Gilić, N. Romčević, Isotope – like effect in YVO4:Eu3+ nanopowders: Raman spectroscopy, J. Raman Spectrosc. 50 (2019) 802–808.
[20] D. Šević, M.S. Rabasović, J. Križan, S. Savić – Šević, M. Mitrić, M. Gilić, B. Hadžić, N. Romčević, Characterization and luminiscence kinetics of Eu^{3+} doped YVO_4 nanopowders, Mater. Res. Bull. 88 (2017) 121–126.
[21] A. Huignard, V. Buissette, A.-C. Franville, T. Gacoin, J.-P. Boilot, Emission processes in YVO4:Eu nanoparticles, J. Phys. Chem. B 107 (2003) 6754–6759.
[22] J. Trajić, M.S. Rabasović, S. Savić – Šević, D. Šević, B. Babić, M. Romčević, J. L. Ristić – Đurović, N. Paunović, J. Križan, N. Romčević, Far – infared spectra of dysprosium doped yttrium aluminum garnet nanopowder, Infrared Phys. Technol. 77 (2016) 226–229.
[23] J.C.M. Garnett, Colours in meta glasses and in metallic films, Philos. Trans. Royal Soc. A 203 (1904) 385–420.
[24] I.J. Uhanov, Opt. Svojstva Poluprovodnikov, Nauka, Moskva, 1977.
[25] C.Z. Bi, J.Y. Ma, J. Yan, X. Fang, D.Z. Yao, B.R. Zhao, X.G. Qiu, Far – infrared optical properties of YVO_4 single crystal, Eur. Phys. J. B 51 (2006) 167–171.
[26] B. Hadžić, N. Romčević, M. Romčević, I. Kuryliszyn – Kudelska, W. Dobrowolski, J. Trajić, D.V. Timotijević, U. Narkiewicz, D. Sibera, Surface optical phonons in ZnO(Co) nanoparticles: Raman study, J. Alloys Compd. 540 (2012) 49–56.
[27] R. Kubrin, Nanophosphor coatings: technology and applications, opportunities and challenges, KONA Powder and Particle Journal 31 (22 – 52) (2014).
[28] T. Thu Huong, H. Thi Phuong, L. Thi Vinh, H. Thi Khuyen, T. Kim Anh, L. Quoc Minh, Functionalized YVO_4:Eu^{3+} nanophosphors with desirable properties for biomedical applications, J. Sci – Adv. Mater Dev. 1 (3) (2016) 295–300.
[29] T. Minakova, S. Mjakin, V. Bakhmetyev, M. Sychov, I. Zyatikov, I. Ekimova, V. Kozik, Y.-W. Chen, I. Kurzina, High efficient $YVPO_4$ luminescent materials activated by europium, Crystals 9 (2019) 658.
[30] H. Zhu, H. Hu, Z. Wang, D. Zuo, Synthesis of YVO4:Eu3+/YBO3 heteronanostructures with enhanced photoluminescence properties, Nanoscale Res. Lett. 4 (2009) 1009–1014.
[31] L. Magnusdottir, A. Uskov, S. Bischoff, J. Mork, Multiphonon capture processes in self-assembled quantum dots, in: Technical Digest. Summaries of Papers Presented at the Quantum Electronics and Laser Science Conference. Postconference Technical Digest (IEEE Cat. No.01CH37172), 2001, pp. 206–207.
[32] R. Liu, L. Liu, Y. Liang, Energy transfer and color – tunable luminescence properties of YVO4:Re (Re = Eu3+, Sm3+, Dy3+, Tm3+) phosphors via molten salt synthesis, Opt. Mater. Express 8 (6) (2018) 1686.